

FROM DIET TO FREE LUNCH: ESTIMATING AUXILIARY SIGNAL PROPERTIES USING DYNAMIC PRUNING MASKS IN SPEECH ENHANCEMENT NETWORKS

Riccardo Miccini^{b‡}, Clément Laroche^b, Tobias Piechowiak^b, Xenofon Fafoutis[#], Luca Pezzarossa[#]

^bGN Hearing [#]Technical University of Denmark (DTU)

ABSTRACT

Speech Enhancement (SE) in audio devices is often supported by auxiliary modules for Voice Activity Detection (VAD), SNR estimation, or Acoustic Scene Classification to ensure robust context-aware behavior and seamless user experience. Just like SE, these tasks often employ deep learning; however, deploying additional models on-device is computationally impractical, whereas cloud-based inference would introduce additional latency and compromise privacy. Prior work on SE employed Dynamic Channel Pruning (DynCP) to reduce computation by adaptively disabling specific channels based on the current input. In this work, we investigate whether useful signal properties can be estimated from these internal pruning masks, thus removing the need for separate models. We show that simple, interpretable predictors achieve up to 93% accuracy on VAD, 84% on noise classification, and an R^2 of 0.86 on F_0 estimation. With binary masks, predictions reduce to weighted sums, inducing negligible overhead. Our contribution is twofold: on one hand, we examine the emergent behavior of DynCP models through the lens of downstream prediction tasks, to reveal what they are learning; on the other, we repurpose and re-propose DynCP as a holistic solution for efficient SE and simultaneous estimation of signal properties.

Index Terms— speech enhancement, speech quality prediction, voice activity detection, edge AI, explainable AI

1. INTRODUCTION

Speech Enhancement (SE) is a fundamental part of many devices aimed at improving communication, collaboration, or quality of life, such as hearing aids, audio wearables, and voice-activated systems. Recent advances in deep learning (DL) have achieved state-of-the-art performance in SE. However, to ensure responsiveness, privacy, and offline operation, DL models must be deployed directly on embedded devices, rather than relying on cloud-based inference. The challenge of running DL models for SE under tight computational constraints has spurred significant research on lightweight architectures such as PercepNet [1], [2], FullSubNet [3], and GTCRN [4].

While SE is often the main component in a speech processing pipeline, real-world solutions may include additional modules for Speech Quality Prediction (SQP), Acoustic Scene Classification (ASC), Signal-to-Noise Ratio (SNR) estimation, or Voice Activity Detection (VAD). These auxiliary elements may be integrated in the SE model or inform downstream business logic, allowing a more seamless, robust, and tailored user experience. For instance, instantaneous SNR or speech quality estimates may provide useful insights to end users, e.g., suggesting them to speak louder or to adjust the

microphone arm when necessary. Indeed, applications of this information to guide hybrid SE systems have been explored extensively: in [2], [5], [6], SNR estimates selectively enable parts of the model; in [7], the authors jointly train for SE and VAD, achieving faster convergence and better performance; in [8], speaker embeddings aid target speaker extraction within a small group of related users; similarly, other signal characteristics such as speaker gender, SNR level, or speech quality have proven useful in zero-shot model selection [9], [10]. While resource-efficient predictors have been investigated, such as those for SQP [11], [12], [13], the computational overhead may still be substantial, even with non-DL methods.

An orthogonal line of research is exploring Dynamic Neural Networks (DynNNs), a class of models which adjust their computation depending on the current input [14]. Several techniques have been recently proposed in the context of speech processing, such as [15], [16], [17]. Among these, Dynamic Channel Pruning (DynCP) [18], [19], [20] involves skipping computation of some of the channels based on an input-dependent criterion, thus adaptively balancing efficiency and performance. In [20], this criterion is expressed by binary masks estimated using gating subnets inserted into each processing block of the SE backbone; see Fig. 2 for an example. In their work, the authors empirically show that those masks seem to correlate with signal characteristics such as noise level or voice activity, raising the following questions: *a*) what information is learned by the gating subnets? *b*) can we exploit it to perform those auxiliary tasks without needing dedicated models?

In this article, we address these questions by drawing from recent literature investigating the latent representations of audio models [21], [22]. In particular, we demonstrate how DynCP gating subnets implicitly learn and encode relevant information about speech and acoustic conditions, despite being trained to efficiently allocate computational resources. By using the binary pruning masks as input features for prediction models, we can perform tasks such as SNR estimation, SQP, VAD, and estimation of other signal properties in real-time, at virtually no extra cost. We deliberately use linear/logistic regression to test whether the information is linearly accessible. These models boast a straightforward formulation, inherently interpretable coefficients, and extremely low computational costs. The latter is further enhanced by the use of binary inputs, which reduces dot-products to simpler gather-and-sum operations, similarly to [12].

Our perspective differs from previous work in three major ways: *a*) instead of training dedicated, compute-heavy SQP models on multiple targets [23], [24], [25], we exploit the DynCP gating subnets as feature extractors; *b*) unlike SE systems where auxiliary cues are explicitly estimated and employed [2], [5], [6], [7], [8], [9], [26], we show how we can extrapolate this information as a byproduct of DynCP, suggesting similarities between DynNNs and multi-task learning; *c*) prior work on audio embeddings focused on continuous representations [21], [22], while work on sparse activations did not tackle audio [27]. We therefore contribute the following: *1*) a pipeline

This work has received funding from the European Union’s Horizon research and innovation program under grant agreement No. 101070374.

Table 1. Overview of ancillary prediction tasks.

Name	Task type	Classes/IQR	Computed from
VAD	Classification	2	Clean energy envelope
Gender	Classification	2	Metadata from VoiceBank [28], [29]
Accent	Classification	6	Metadata from VoiceBank [28], [29]
Noise category	Classification	6	Metadata from VBD+D [30] and DEMAND [31]
Input SNR	Regression	-13-8 dB	librosa.feature.rms
Enhanced SNR	Regression	1-14 dB	librosa.feature.rms
Input SI-SDR	Regression	-1-10 dB	auraloss.time.SISDRLoss
Enhanced SI-SDR	Regression	8-17 dB	auraloss.time.SISDRLoss
Input PESQ	Regression	1.2-1.7	torch_pesq.PesqLoss.mos
Enhanced PESQ	Regression	2.6-2.9	torch_pesq.PesqLoss.mos
F_0	Regression	110-200 Hz	pyworld.dio and pyworld.stonemask

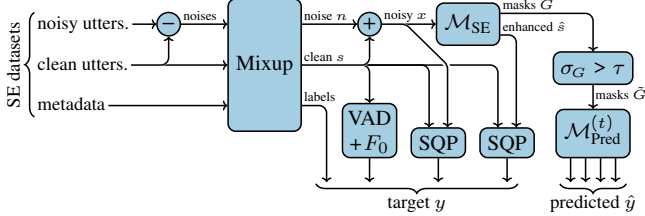


Fig. 1. Overview of the proposed system, showing data generation pipeline, SE model, targets extraction, and prediction models.

for computing and aligning DynCP masks with auxiliary speech and acoustic attributes; 2) performance evaluation across multiple classification, regression, and Speaker Verification (SV) tasks; 3) extensive analyses and visualizations of the emergent behavior of DynCP SE models, with the hope of encouraging further research in this area.

2. METHODS

The proposed system is illustrated in Fig. 1. At its core, our work involves estimating $y_l^{(t)} \forall t \in \mathbb{T}$, where \mathbb{T} is the set of prediction targets¹ (summarized in Table 1) and l represents the current time step. Since the SE model considered here operates in the Short-Time Fourier Transform (STFT) domain, each time step l corresponds to a frame of window length w and hop size h . Accounting for the time dimension, our problem becomes:

$$y^{(t)} \approx \hat{y}^{(t)} = \mathcal{M}_{\text{Pred}}^{(t)}(\tilde{G}); \quad y^{(t)} \in \begin{cases} \mathbb{R}^L & \text{regression} \\ \{0, 1\}^L & \text{classification} \end{cases} \quad (1)$$

where L is length of the input sequence, $\mathcal{M}_{\text{Pred}}^{(t)}$ is the model associated with target t , consisting of a set of coefficients, and \tilde{G} is a matrix containing the pruning masks to be used as input features.

2.1. Data Pipeline

SE models are usually trained on batches of clean-noisy pairs, often corresponding to single utterances. Since we are interested in real-time streaming use cases, we treat our training and test data as one long continuous signal. As shown in Fig. 1, this is achieved by first extracting the individual noise excerpts from the noisy utterances. Subsequently, we generate the clean speech and noise signals s and n by picking utterances/excerpts in random order. Lastly, we mix them to form the noisy signal x . The noisy mixture x is then processed by the DynCP SE model, yielding the enhanced speech signal \hat{s} . To ensure a fair evaluation and avoid data leakage, we assign different

¹Here, we use “target” for a given signal characteristic or class label and “task” for the associated prediction problem, often comprising multiple targets. Since linear model coefficients can be concatenated into a single matrix, we treat the two terms somewhat interchangeably.

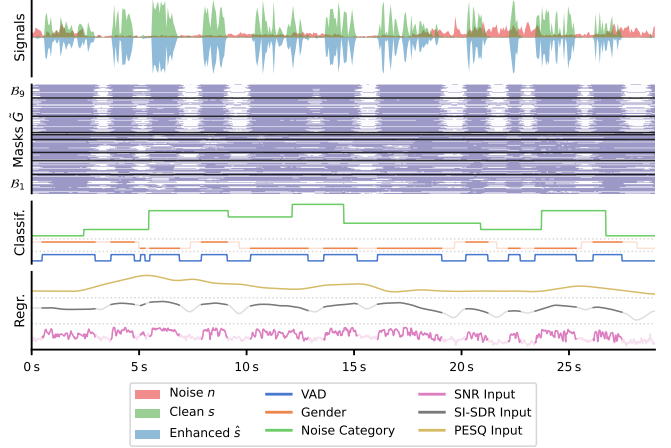


Fig. 2. Example generated data, showing clean/noise/enhanced audio, binary pruning masks, and a selection of ground truths; for relevant targets, we highlight regions with voice activity.

speakers to the train and test splits and sample individual utterances using a stratified scheme that maintains a uniform distribution of gender and accent classes; we apply the same stratification strategy to the noise categories. The audio signals are further processed to extract the ground truths for the regression tasks, while the binary pruning masks are gathered from the internal gating subnets. See Fig. 2 for an example of the aforementioned generated data.

2.2. Speech Enhancement with Dynamic Channel Pruning

We employ Conv-FSENet, introduced in [20], as our DynCP model for SE. It is a STFT-domain model comprising $\{\mathcal{B}_i\}_{i=1}^I$ processing blocks chained in series, each governed by a separate gating subnet. The primary output of the model is the suppression mask \hat{M} , used to recover the enhanced speech spectrum \hat{S} from noisy mixture X :

$$S_{l,f} \approx \hat{S}_{l,f} = \hat{M}_{l,f} X_{l,f}; \quad \hat{M} \in \mathbb{R}^{L \times F}; \quad X, S, \hat{S} \in \mathbb{C}^{L \times F} \quad (2)$$

where L and F , indexed by l and f , are the number of time steps and frequency bins, respectively. The model additionally produces a tensor of binary pruning masks G determining which of the C_{res} convolutional channels in each block are active. Thus, we have:

$$\hat{M}, G = \mathcal{M}_{\text{SE}}(X); \quad G \in \{0, 1\}^{L \times I \times C_{\text{res}}} \quad (3)$$

Although G contains too much data to be viable as input features, not all of its masks are equally useful. In fact, during training, the gating subnets might learn to treat certain channels as always needed or always unnecessary. As a result, some of the masks in G are constant or quasi-constant; such features would obviously be uninformative, so we filter them out by enforcing a minimum standard deviation τ , resulting in a subset of $C^* \leq IC_{\text{res}}$ features:

$$\tilde{G} := \{G_{:,i,c} \mid \sigma_{G_{:,i,c}} > \tau\}; \quad \tilde{G} \in \{0, 1\}^{L \times C^*} \quad (4)$$

2.3. Targets Extraction

The ground truths for the prediction tasks, listed in Table 1, can be divided into discrete and continuous. Some of the discrete targets are based on dataset metadata; when sampling utterances and noises to form s and x , we also retrieve their corresponding metadata and append them to a time series whose time resolution matches that of the

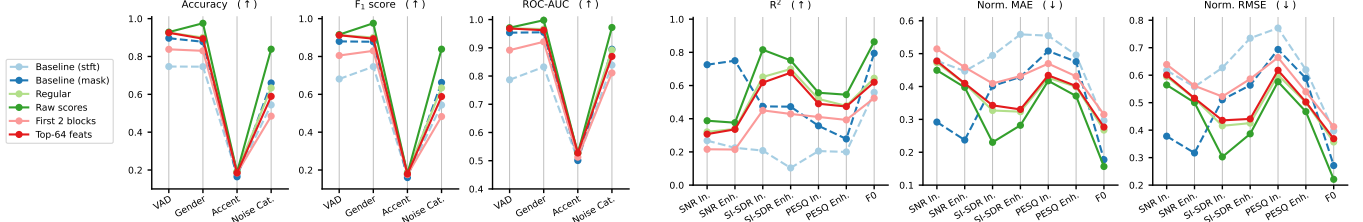


Fig. 3. Performance on each task using different input features (colors); first 3 subplots show classification, last 3 subplots show regression.

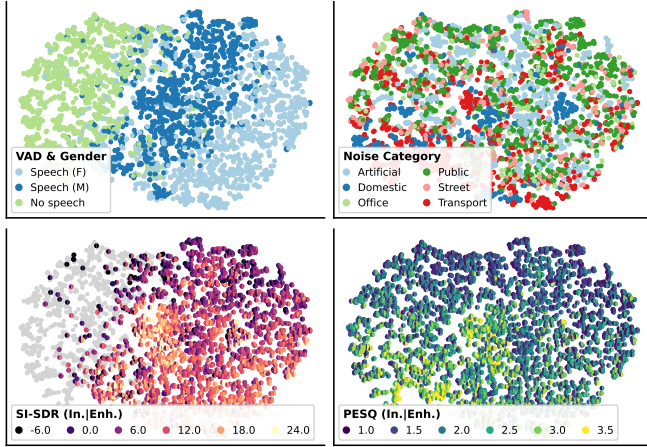


Fig. 4. Low-dimensional visualization of pruning masks, computed using t-SNE; for each subplot, points are colored by different targets.

STFT frames. To estimate the VAD target, we: *1*) compute the Root Mean Square (RMS) for each window; *2*) apply a zero-phase simple moving average filter; *3*) binarize the resulting energy envelope signal according to a threshold; *4*) smooth and binarize the coarse estimate again to obtain the final ground truth.

The continuous regression targets comprise speech quality metrics extracted from both noisy and enhanced signals using the SQP modules shown in Fig. 1; these metrics are: *a*) SNR, computed per-frame using the aforementioned RMS signals; *b*) Scale-Invariant Signal-to-Distortion Ratio (SI-SDR) [32], computed on 1 s windows with 75 % overlap; *c*) Perceptual Evaluation of Speech Quality (PESQ) [33], computed on 3 s windows with 75 % overlap, padded with 0.5 s of silence on both ends; SNR and SI-SDR values are converted to dB and clamped between -50 dB and 30 dB. To match the time resolution of the other ground truths, we upsample the SI-SDR and PESQ targets to the STFT frame rate by interpolating them using a squared-Hann window. We also extract the fundamental frequency F_0 of the clean speech using the WORLD vocoder [34], with a frame period matching the STFT hop size h .

3. EXPERIMENTAL SETUP

Data generation We use the speech utterances and noise excerpts from VoiceBank+DEMAND (VB+D) [30], combining all of its 88 English and non-English speakers. Since the speech data in VB+D is taken from VoiceBank (VB) [28], [29], we use its metadata for gender and accent labels. Noise classes are based on the noise types reported in VB+D and matched with the categories listed in DEMAND [31]; an additional “Artificial” class is used to describe custom noises. We keep the 5 most common accent classes and merge the rest into class “Other”. We retain the original gain of the noise

excerpts, which offered a sufficient level of SNR variability. We withheld 27 speakers for testing, i.e., ~ 30 % of the total. This resulted in 30 min of training data (600 utterances, for a total of 112 563 datapoints) and 30 min of testing data (594 utterances, totaling 112 716 datapoints). The SE backbone is parameterized with $C_{\text{res}} = 128$ convolutional channels and $I = 9$, i.e., 3 stacks with 3 blocks each. The DynCP gating subnets feature 16 hidden channels and pooling over the entire receptive field. The model is trained as described in [20] with 0.25 target utilization and surrogate gradients. We apply a threshold $\tau = 0.005$ to the standard deviation of the masks, resulting in $C^* = 202$ features (~ 18 % of all channels).

Alternative features We included the noisy input STFT log-magnitude and the predicted suppression mask \tilde{M} as baselines; both comprise 257 features. As additional experiments, we also trained the prediction models on: *a*) features from the first 2 blocks only (67 in total); *b*) top-64 most informative features based on their linear coefficients on the regular setup; *c*) pruning scores \tilde{R} , i.e., the raw outputs of the gating subnets before binarization; for consistency, we keep the same channels and dimensionality as \tilde{G} . We apply z-score normalization to any non-binary variant, i.e., input spectrograms, predicted suppression masks, and raw pruning scores.

Prediction models We employ logistic and linear regression models for classification and regression tasks, respectively. We apply ℓ_2 (Tikhonov) regularization with a factor $\alpha = 0.01$ to account for feature collinearity. We evaluate classification performance by accuracy, F_1 -score, and Area Under the Receiver Operating Characteristic Curve (ROC-AUC). For regression, we use Coefficient of Determination (R^2), Mean Absolute Error (MAE), and Root Mean Square Error (RMSE); to simplify comparison across tasks, we normalize the two latter metrics by the interquartile ranges shown in Table 1. Both metrics and models rely on the `scikit-learn` library. Lastly, gender/accent classification and SNR/SI-SDR regression are trained and evaluated only on frames with voice activity (~ 68 % of all data), using the VAD target as oracle. Similarly, fundamental frequency estimation only employs frames where $F_0 \neq 0$.

Speaker Verification (SV) We explore the viability of pruning masks as embeddings for SV. For each utterance $u \in \mathcal{U}$, we define $\tilde{G}^{(u \wedge v)}$ as the subset of mask frames from utterance u featuring voice activity, implied by v . Each subsequence is then averaged and ℓ_2 -normalized, yielding the set \mathcal{E} of utterance-level embeddings e :

$$\mathcal{E} := \left\{ \frac{\tilde{G}^{(u)}}{\|\tilde{G}^{(u)}\|_2} \mid u \in \mathcal{U} \right\}; \quad \tilde{G}^{(u)} = \mathbb{E}_l [\tilde{G}^{(u \wedge v)}] \quad (5)$$

where \mathcal{U} is the set of all utterances and $\tilde{G}^{(u)}$ is the average across time of each aforementioned subsequence. We employ a standard linear backend consisting of Within-Class Covariance Normalization (WCCN) and Linear Discriminant Analysis (LDA) (with 16 output dimensions) followed by length normalization and cosine similarity for scoring, similar to [35]. We fit the backend on the training split and

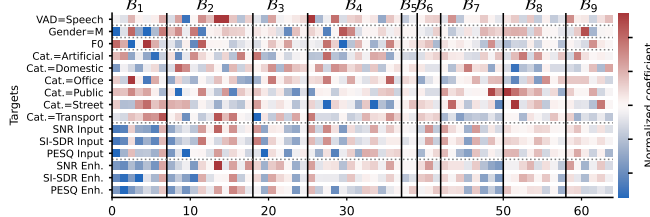


Fig. 5. Normalized coefficients (red for positive, blue for negative) for models trained on the top-64 most informative features (x-axis, grouped by processing block); showing a subset of targets (y-axis).

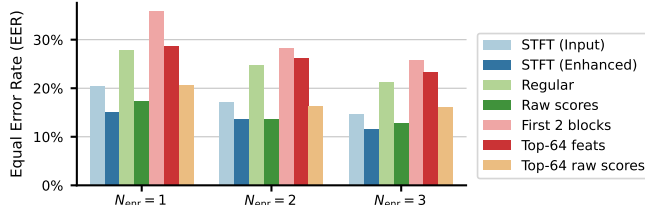


Fig. 6. SV performance across different number of enrollment utterances (x-axis) and feature sets (colors).

evaluate on the test data. For each speaker, we assign $N_{\text{enr}} \in \{1, 2, 3\}$ embeddings from \mathcal{E} as enrollment (averaging them when $N_{\text{enr}} > 1$) and perform verification trials on the remaining ones. We generate pairs of enrollment and test utterances with a 1:10 ratio of target and non-target speakers, totaling between 5670 and 5130 trials depending on N_{enr} . Lastly, we omit the suppression mask baseline and instead show the enhanced STFT log-magnitude and the top-64 most informative raw pruning scores. As customary for SV, we evaluate performance using the Equal Error Rate (EER).

4. RESULTS

Fig. 3 compares predictors trained on features from DynCP against baseline data. Regular binary masks (●) outperform both baselines across most classification and regression tasks, with the 64 most informative features (●) retaining the same performance as the full set (●), suggesting that auxiliary models can be very compact. Conversely, only using data from the first two blocks (●) causes a significant performance drop, potentially implying that the gating subnets learn progressively more complex features throughout the blocks. Raw scores (●) are strongest on nearly all tasks, with the highest gains in noise classification and input SI-SDR/ F_0 estimation; this is expected, as they carry more information about the internal state of the SE model. Accent is remarkably hard to predict, with near-chance performance across all variants, plausibly because SE behavior is not particularly affected by this factor. Lastly, the \hat{M} baseline (●) dominates tasks with rapidly varying targets such as SNR or F_0 . In these cases, features from DynCP models are inherently penalized, due to the temporal averaging occurring inside the gating subnets.

Using the top-32 principal components of 20% of the binary pruning masks in the test set, we fit a t-SNE manifold to visualize them in a low-dimensional space. As evidenced in Fig. 4, the signal characteristics are arranged in a semantically meaningful way. In particular, we observe distinct clusters for voice activity, with secondary separation by speaker gender and continuous gradients for SI-SDR and PESQ. Interestingly, a closer inspection of input and enhanced labels reveals slightly different trajectories between targets, with these trends extending into noise-only regions in the case of

PESQ. Somewhat unexpectedly, noise categories fragment into smaller, scattered clusters: indeed, the metadata used as labels mostly describe the recording environment rather than the actual noise content.

The heatmap in Fig. 5 shows how each pruning mask contributes to the estimation of the different targets. It comprises coefficients of models trained on the top-64 binary features (● in Fig. 3). To simplify comparison across different tasks and value ranges, we normalize them by first multiplying them by the standard deviation of their respective input features and then scaling to unit ℓ_2 -norm. Once again, several trends emerge; intuitively, features driving male classification overlap with those used for fundamental frequency regression, albeit with opposite polarity, consistent with known gender-pitch correlation. Conversely, in noise category classification, classes rely on disjoint subsets of features, with the few shared ones having different polarity. Meanwhile, SNR, SI-SDR, and PESQ — although to a lesser extent — rely on overlapping sets of features, with many belonging to the earlier blocks and featuring negative coefficients. These observations may be taken as evidence that the underlying DynCP SE model learns to behave conservatively, only activating the channels associated with those masks when the input signal is particularly noisy. Lastly, and rather counterintuitively, some VAD/gender-relevant features also appear to inform noise classification, which could indicate occasional confusion between background and target speech.

The results of our last set of experiments, tackling SV, are shown in Fig. 6. Using our relatively simple setup, the DynCP masks achieve only modest EER. This is particularly true for binary features (●, ●, and ●), mostly ranking worse than the STFT baselines (● and ●). Nevertheless, the full set of raw scores (●) performs similarly, while requiring 21 % fewer operations; dropping the number of features to 64 (●), however, heavily degrades performance. It is unclear whether the lackluster results are due to information loss from temporal pooling, or because the underlying SE model learns an internal representation that is mostly speaker-agnostic, thereby abstracting away individual speaker characteristics.

5. CONCLUSION

We showed that the binary pruning masks learned by a DynCP SE model expose linearly accessible information about speech and acoustic properties of its input, hinting at local competition inside the model [27]. With as few as 64 features, we achieve 93 % accuracy on VAD and 59 % on noise classification; when predicting input PESQ and SI-SDR, we obtain a MAE of 0.2 and 3.2 dB, respectively. Most crucially, these auxiliary estimates come with almost negligible computational overhead; when considering all classification and regression tasks (totaling 21 targets) on the full set of 202 features, we only incur 4242 additional arithmetic operations per frame, i.e., somewhere between 0.6 % and 0.93 % of the total compute, depending on the number of currently active channels.

While far from mature, our preliminary results pave the way for DynCP-based single-model pipelines capable of simultaneously enhancing speech, saving compute, and producing auxiliary data that can aid robustness and user experience. Nonetheless, we point out the following limitations: *a*) linear models assume additive contributions and are sensitive to correlated inputs; *b*) collinearity between features makes interpretation of model coefficients as feature *importance* difficult and potentially misleading; *c*) temporal smoothing may hinder estimation of quickly-changing targets; *d*) the windowed PESQ ground truths adopted here might not be fully representative of the instantaneous signal quality. As part of our research, we plan to investigate other types of dynamic models, and experiment with simultaneously training on SE and auxiliary tasks.

6. REFERENCES

[1] J.-M. Valin, U. Isik, N. Phansalkar, R. Giri, K. Helwani, and A. Krishnaswamy, “A Perceptually-Motivated Approach for Low-Complexity, Real-Time Enhancement of Fullband Speech,” in *Interspeech 2020*, Oct. 2020.

[2] X. Ge, J. Han, Y. Long, and H. Guan, “PercepNet+: A Phase and SNR Aware PercepNet for Real-Time Speech Enhancement,” in *Interspeech 2022*, Sep. 2022, arXiv: 2203.02263 [eess].

[3] X. Hao, X. Su, R. Horaud, and X. Li, “Fullsubnet: A Full-Band and Sub-Band Fusion Model for Real-Time Single-Channel Speech Enhancement,” in *ICASSP 2021 - 2021 IEEE International Conference on Acoustics, Speech and Signal Processing (ICASSP)*, Jun. 2021.

[4] X. Rong, T. Sun, X. Zhang, Y. Hu, C. Zhu, and J. Lu, “GTCRN: A Speech Enhancement Model Requiring Ultralow Computational Resources,” in *ICASSP 2024 - 2024 IEEE International Conference on Acoustics, Speech and Signal Processing (ICASSP)*, Apr. 2024.

[5] S. Lv, Y. Hu, S. Zhang, and L. Xie, “DCCRN+: Channel-Wise Subband DCCRN with SNR Estimation for Speech Enhancement,” in *Interspeech 2021*, Aug. 2021, arXiv: 2106.08672 [eess].

[6] H. Schröter, A. N. Escalante-B, T. Rosenkranz, and A. Maier, “Deep-FilterNet: Perceptually Motivated Real-Time Speech Enhancement,” in *24th Annual Conference of the International Speech Communication Association, Interspeech 2023, Dublin, Ireland, August 20-24, 2023*, 2023, arXiv: 2305.08227 [eess].

[7] Y. Zhang, H. Zou, and J. Zhu, “VSANet: Real-time Speech Enhancement Based on Voice Activity Detection and Causal Spatial Attention,” arXiv: 2310.07295 [eess], pre-published.

[8] T.-A. Hsieh and M. Kim, “TGIF: Talker Group-Informed Familiarization of Target Speaker Extraction,” arXiv: 2507.14044 [eess], pre-published.

[9] A. Sivaraman and M. Kim, “Sparse Mixture of Local Experts for Efficient Speech Enhancement,” in *Interspeech 2020*, Oct. 2020.

[10] R. E. Zezario, C.-S. Fuh, H.-M. Wang, and Y. Tsao, “Speech Enhancement with Zero-Shot Model Selection,” in *2021 29th European Signal Processing Conference (EUSIPCO)*, Aug. 2021.

[11] F. Cumlin, X. Liang, V. Ungureanu, C. K. A. Reddy, C. Schüldt, and S. Chatterjee, “DNSMOS Pro: A Reduced-Size DNN for Probabilistic MOS of Speech,” in *Interspeech 2024*, Sep. 2024.

[12] M. Nilsson, R. Miccini, C. Laroche, T. Piechowiak, and F. Zenke, “Resource-Efficient Speech Quality Prediction through Quantization Aware Training and Binary Activation Maps,” in *Interspeech 2024*, Sep. 2024, arXiv: 2407.04578 [cs, eess].

[13] M. Nilsson, R. Miccini, J. Rossbroich, C. Laroche, T. Piechowiak, and F. Zenke, “Efficient Streaming Speech Quality Prediction with Spiking Neural Networks,” in *Interspeech 2025*, Aug. 2025.

[14] Y. Han, G. Huang, S. Song, L. Yang, H. Wang, and Y. Wang, “Dynamic Neural Networks: A Survey,” *IEEE Transactions on Pattern Analysis and Machine Intelligence*, Nov. 2022.

[15] R. Miccini, M. Kim, C. Laroche, L. Pezzarossa, and P. Smaragdis, “Adaptive Slimming for Scalable and Efficient Speech Enhancement,” in *2025 IEEE Workshop on Applications of Signal Processing to Audio and Acoustics (WASPAA)*, Oct. 2025, arXiv: 2507.04879 [eess].

[16] M. Elminshawi, S. R. Chetupalli, and E. A. P. Habets, “Dynamic Slimmable Networks for Efficient Speech Separation,” arXiv: 2507.06179 [eess], pre-published.

[17] K. F. Olsen et al. “Knowing When to Quit: Probabilistic Early Exits for Speech Separation,” arXiv: 2507.09768 [cs], pre-published.

[18] Z. Jelčicová, R. Jones, D. T. Blix, M. Verhelst, and J. Sparsø, “PeakRNN and StatsRNN: Dynamic Pruning in Recurrent Neural Networks,” in *2021 29th European Signal Processing Conference (EUSIPCO)*, Aug. 2021.

[19] L. Cheng, A. Pandey, B. Xu, T. Delbrück, and S.-C. Liu, “Dynamic gated recurrent neural network for compute-efficient speech enhancement,” in *Interspeech 2024*, Sep. 2024.

[20] R. Miccini, C. Laroche, T. Piechowiak, and L. Pezzarossa, “Scalable Speech Enhancement with Dynamic Channel Pruning,” in *2025 IEEE International Conference on Acoustics, Speech and Signal Processing (ICASSP)*, Apr. 2025.

[21] F. Cumlin, X. Liang, V. Ungureanu, C. K. A. Reddy, C. Schüldt, and S. Chatterjee, “Impairments are Clustered in Latents of Deep Neural Network-based Speech Quality Models,” in *ICASSP 2025 - 2025 IEEE International Conference on Acoustics, Speech and Signal Processing (ICASSP)*, Apr. 2025.

[22] V. Deng, C. Wang, G. Richard, and B. McFee, “Investigating the Sensitivity of Pre-trained Audio Embeddings to Common Effects,” in *ICASSP 2025 - 2025 IEEE International Conference on Acoustics, Speech and Signal Processing (ICASSP)*, Apr. 2025.

[23] A. Kumar et al., “Torchaudio-Squim: Reference-Less Speech Quality and Intelligibility Measures in Torchaudio,” in *ICASSP 2023 - 2023 IEEE International Conference on Acoustics, Speech and Signal Processing (ICASSP)*, Jun. 2023.

[24] Z. Zhang, P. Vyas, X. Dong, and D. S. Williamson, “An End-To-End Non-Intrusive Model for Subjective and Objective Real-World Speech Assessment Using a Multi-Task Framework,” in *ICASSP 2021 - 2021 IEEE International Conference on Acoustics, Speech and Signal Processing (ICASSP)*, Jun. 2021.

[25] R. E. Zezario, S.-W. Fu, F. Chen, C.-S. Fuh, H.-M. Wang, and Y. Tsao, “Deep Learning-Based Non-Intrusive Multi-Objective Speech Assessment Model With Cross-Domain Features,” *IEEE/ACM Transactions on Audio, Speech, and Language Processing*, 2023, arXiv: 2111.02363 [cs, eess].

[26] X. Tan and X.-L. Zhang, “Speech Enhancement Aided End-To-End Multi-Task Learning for Voice Activity Detection,” in *ICASSP 2021 - 2021 IEEE International Conference on Acoustics, Speech and Signal Processing (ICASSP)*, Jun. 2021.

[27] R. K. Srivastava, J. Masci, F. J. Gomez, and J. Schmidhuber, “Understanding Locally Competitive Networks,” in *3rd International Conference on Learning Representations, ICLR 2015*, May 2015, arXiv: 1410.1165 [cs].

[28] C. Veaux, J. Yamagishi, and S. King, “The voice bank corpus: Design, collection and data analysis of a large regional accent speech database,” in *2013 International Conference Oriental COCOSDA Held Jointly with 2013 Conference on Asian Spoken Language Research and Evaluation (O-COCOSDA/CASLRE)*, Nov. 2013.

[29] J. Yamagishi, C. Veaux, and K. MacDonald, *CSTR VCTK Corpus: English Multi-speaker Corpus for CSTR Voice Cloning Toolkit*, version 0.92, Nov. 2019.

[30] C. Valentini-Botinhao, X. Wang, S. Takaki, and J. Yamagishi, “Investigating RNN-based speech enhancement methods for noise-robust Text-to-Speech,” in *9th ISCA Workshop on Speech Synthesis Workshop (SSW 9)*, Sep. 2016.

[31] J. Thiemann, N. Ito, and E. Vincent, *Demand: A Collection Of Multi-Channel Recordings Of Acoustic Noise In Diverse Environments*, Jun. 2013.

[32] J. Le Roux, S. Wisdom, H. Erdogan, and J. R. Hershey, “SDR – Half-baked or Well Done?” in *ICASSP 2019 - 2019 IEEE International Conference on Acoustics, Speech and Signal Processing (ICASSP)*, May 2019.

[33] A. Rix, J. Beerends, M. Hollier, and A. Hekstra, “Perceptual Evaluation of Speech Quality (PESQ) - a New Method for Speech Quality Assessment of Telephone Networks and Codecs,” in *2001 IEEE International Conference on Acoustics, Speech, and Signal Processing*, May 2001.

[34] M. Morise, F. Yokomori, and K. Ozawa, “WORLD: A Vocoder-Based High-Quality Speech Synthesis System for Real-Time Applications,” *IEICE Transactions on Information and Systems*, 2016.

[35] N. Dehak, P. J. Kenny, R. Dehak, P. Dumouchel, and P. Ouellet, “Front-End Factor Analysis for Speaker Verification,” *IEEE Transactions on Audio, Speech, and Language Processing*, May 2011.